EUROPEAN ORGANIZATION FOR NUCLEAR RESEARCH

CERN – A&B DEPARTMENT

AB-Note-2005-042 RF

Simulation of Longitudinal and Transverse Impedances of Trapped Modes in LHC Secondary Collimator

A. Grudiev

Abstract

The results of simulation of trapped modes in LHC (phase 1) secondary collimators are presented. Both monopole and dipole modes have been analyzed giving estimates of the longitudinal and transverse impedances for different values of the collimator gap. The comparison with available measurement data shows good agreement. It has been found that a monopole mode at 1.25 GHz gives the main contribution to the longitudinal impedance resulting mainly in heat deposition in the region of sliding RF finger. Estimated maximum losses are 65 mW per finger for nominal LHC beam intensity. Several dipole modes which give non-negligible contribution to the transverse impedance at frequencies below 2 GHz have been found and analyzed.

Keywords: Collimator impedances, longitudinal impedance, transverse impedance, trapped modes.

30th November 2005
Geneva, Switzerland

INTRODUCTION

In this note, the results of a study of trapped modes in the LHC secondary collimator which will be used in early operation period (phase 1) and which we refer to as collimator in this text are presented. Since the mechanical design existed already [1], the main question addressed in the study is to identify and to quantify trapped mode impedance related problems which can harm LHC operation and/or the collimator itself. The geometry of the collimator used in the simulations corresponds to that of the prototype built and tested in the SPS [2].

In Fig. 1, the geometry of the collimator is shown as it is represented in HFSS (frequency domain RF code) [3], which has been used for 3D-model input and eigenmode calculations. Since only 1/8 of the collimator has been calculated in order to save computation resources, different boundary conditions have been applied on the three symmetry planes depending on the type of modes under study. This geometry has been transferred from HFSS to GdfidL [4], a time domain code, which has been used to calculate wakefields and impedances.

The collimator geometry is quite complicated. It comprises a vacuum tank, moveable plates, RF fingers and a region of transition from plates to beam pipe (see [1] for details). All these parts form a cavity of very complex shape, which can be considered as an RF resonator where a large number of modes are trapped. Direct calculation of all modes one by one using HFSS is very time consuming. We have used another approach combining time domain calculation of impedance using GdfidL for identification of frequencies of the relevant modes, and a subsequent accurate calculation of the parameters of the identified modes in frequency domain using HFSS.

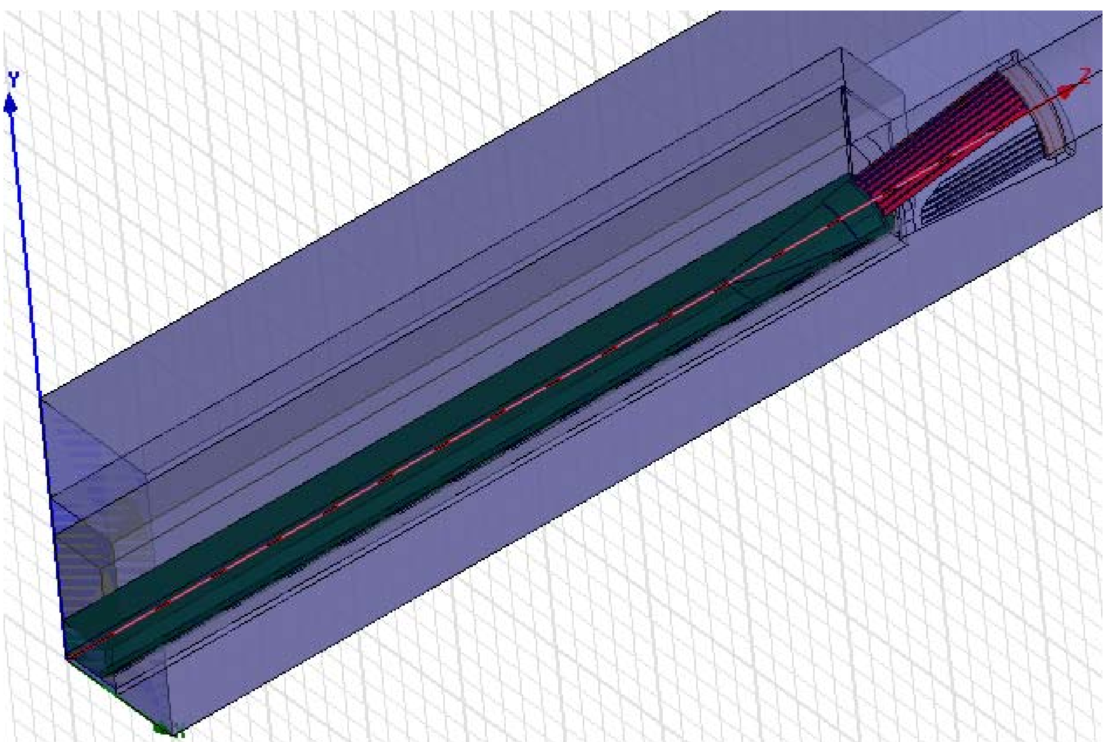

FIGURE 1. Geometry of the collimator as represented in HFSS.

a)

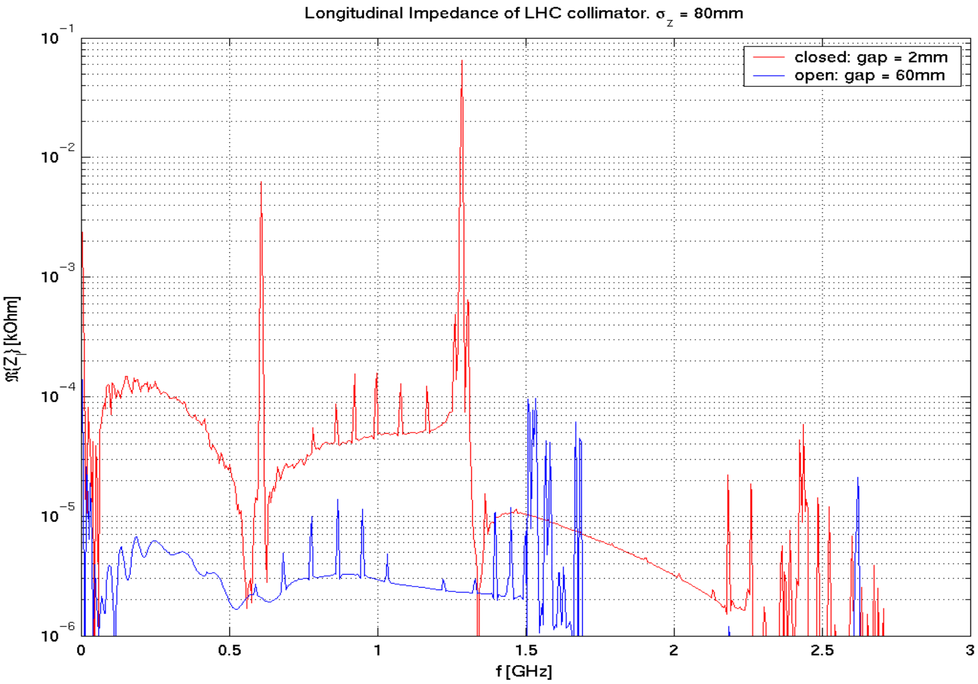

b)

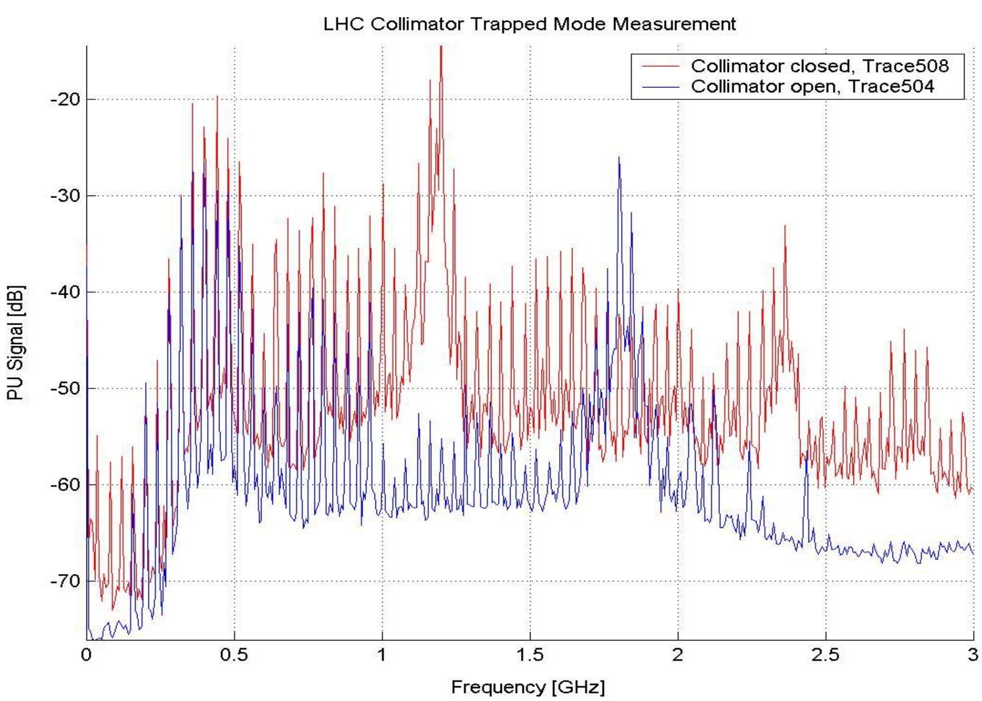

FIGURE 2. a): Real part of the effective impedance for two gap values: 2 mm and 60 mm, in red and blue, respectively. b): Results of the measurements made by F. Caspers and T. Kroyer in the SPS [4].

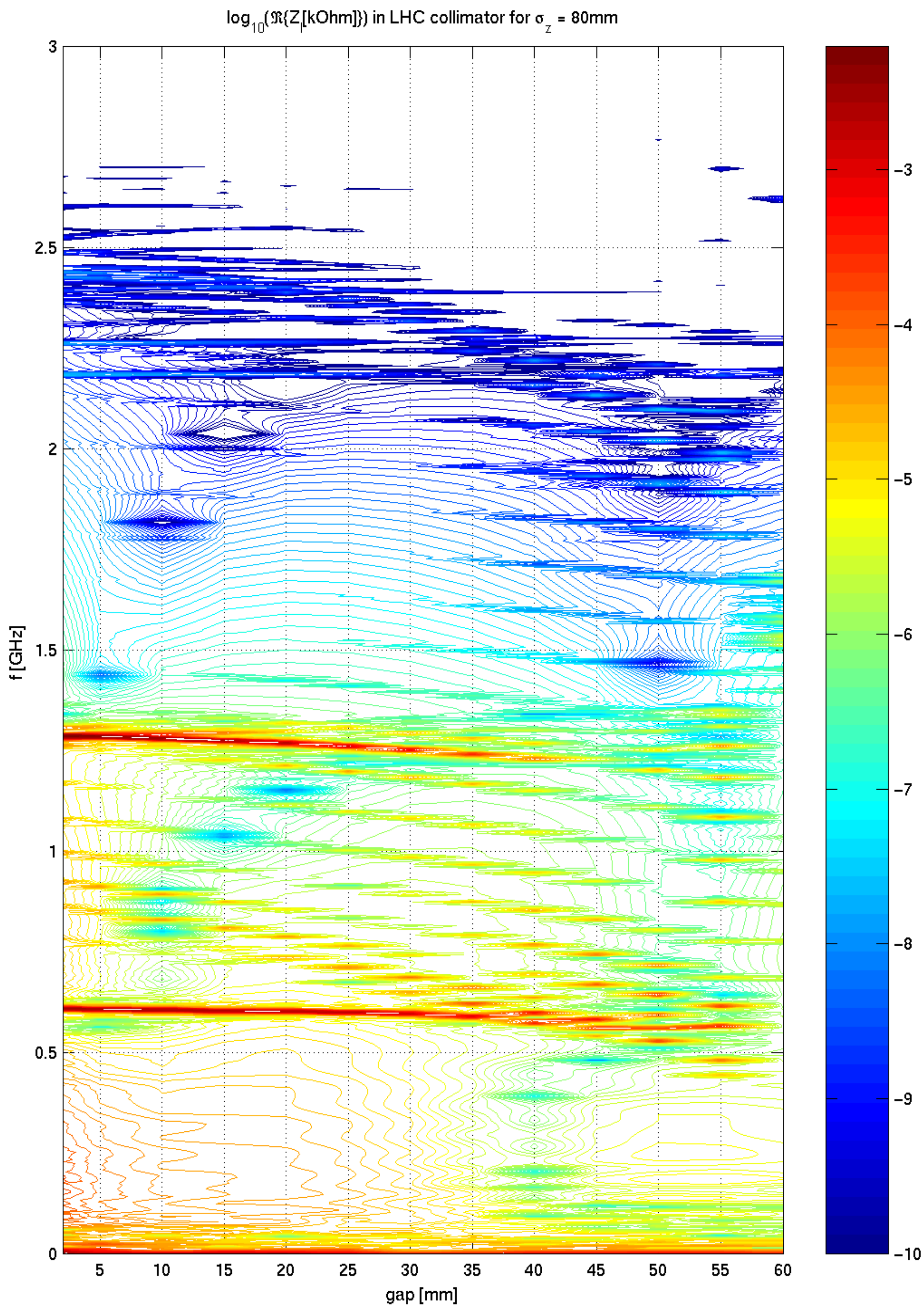

FIGURE 3. Map of effective longitudinal impedance is presented in the range of frequencies from DC to 3 GHz and in the range of gaps from 2 mm to 60 mm.

a)

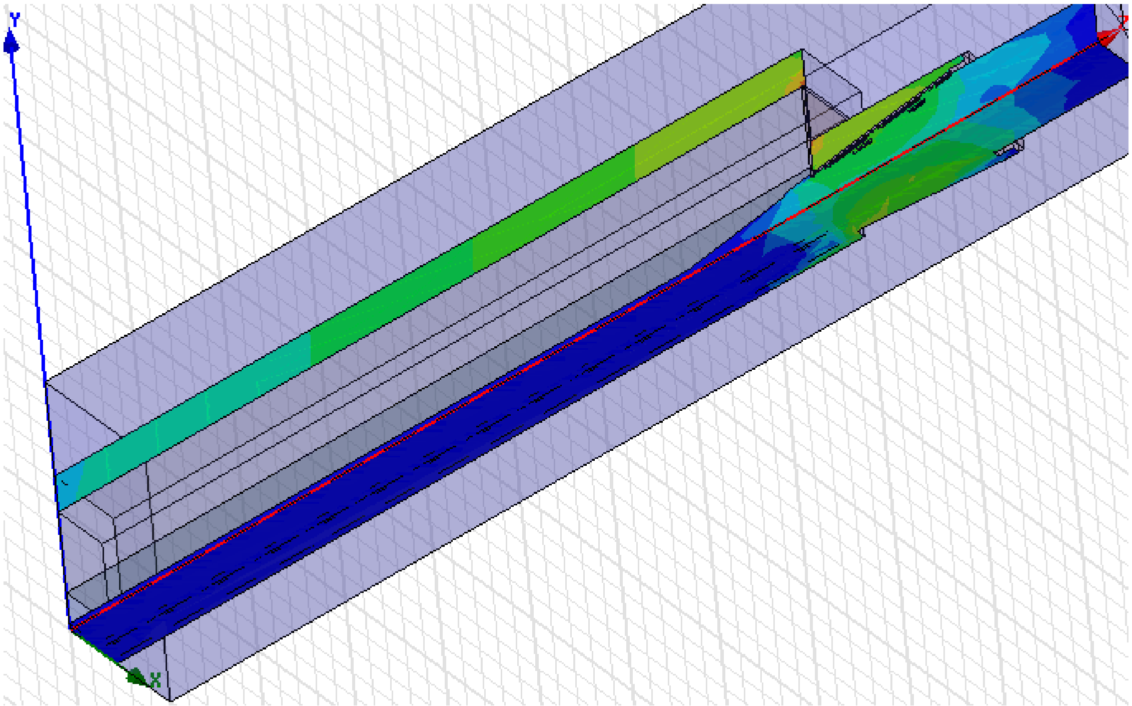

b)

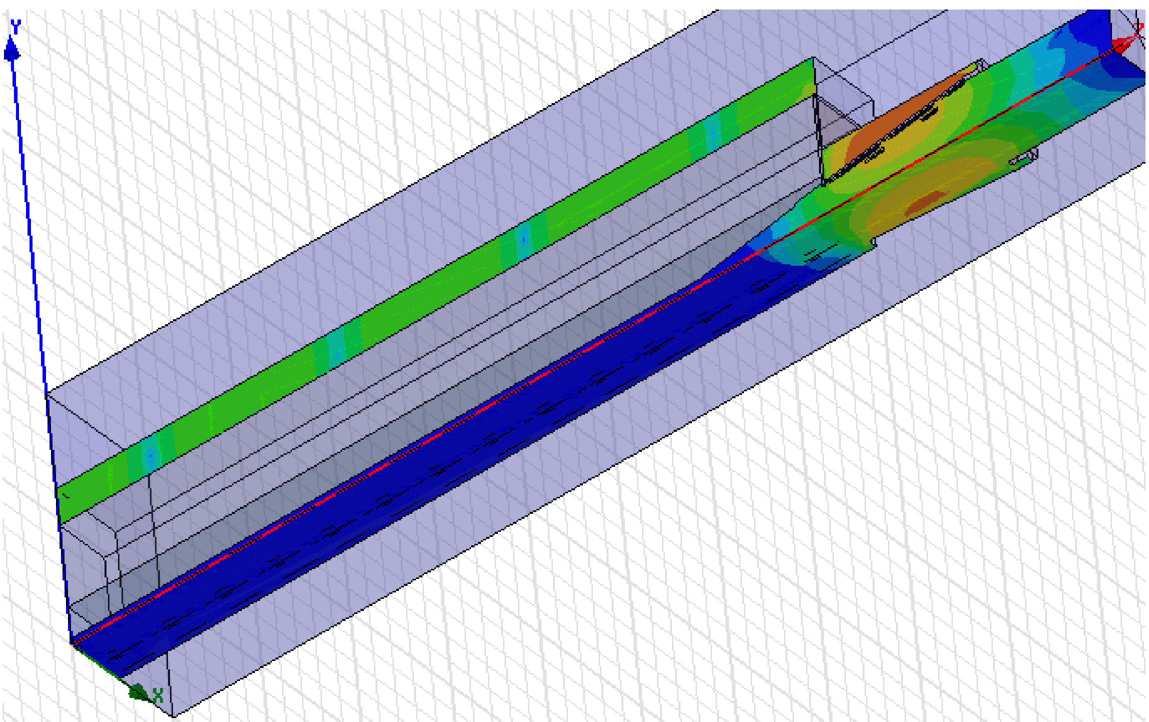

FIGURE 4. Electric field distribution of the first (a) and the second (b) dominant modes.

LONGITUDINAL IMPEDANCE OF MONOPOLE MODES

Appling the perfect magnetic wall ($H_t = 0$) boundary condition both on $x = 0$ and $y = 0$ symmetry planes of the collimator geometry presented in Fig. 1, monopole modes ($m = 0$) have been calculated. First, the effective longitudinal impedance, i.e. the impedance taking into account coupling to a Gaussian bunch of 80 mm RMS length, has been calculated using GdfidL for about 10 different values of the gap between the collimator plates from 2 mm (the smallest gap) to 60 mm (collimator fully open). The real part of the effective impedance is presented in Fig. 2(a) for two gap values: 2 mm and 60 mm, in red and blue, respectively. In Fig. 2(b), the results of the measurements made in the SPS [2] are also presented for comparison. The numerical and experimental results are in a good agreement. Moreover, in Fig. 3, a map of the effective longitudinal impedance is presented in the range of frequencies from DC to 3 GHz and in the range of gaps from 2 mm to 60 mm. The impedance map shows two modes at about 0.6 GHz and 1.25 GHz to be dominant. Knowing their frequencies, the electromagnetic fields and parameters of these dominant modes have been calculated using HFSS for the gap values of 10 mm. In Fig. 4, the electric field distribution of these modes is shown. According to the second mode's field distribution shown in Fig. 4(b) the losses are concentrated mainly in the transition region where the RF fingers are situated. Thus potential overheating of the RF fingers is the main concern.

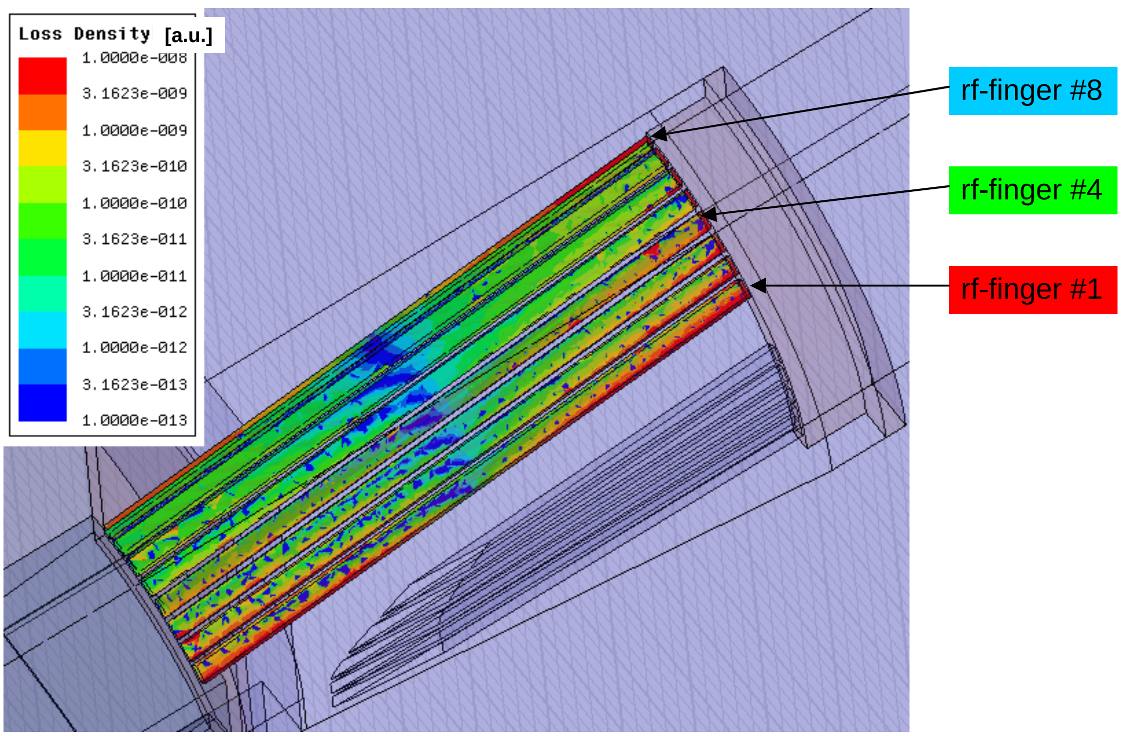

FIGURE 5. Loss density distribution on the surface of rf fingers for the second mode.

Table 1 summarizes the parameters of these two dominant modes. In the last row of the table, an upper estimate of the power losses induced in the whole collimator by the nominal LHC beam (bunch charge: $q = 16\,\mathrm{nC}$, bunch spacing: $t_b = 25\,\mathrm{ns}$, and RMS bunch length: $\sigma_z \approx 80\,\mathrm{mm}$) for each mode is presented, assuming that the mode frequency coincides with one of the beam harmonics, where $P_{loss} = (q/t_b)^2 r_l \exp\left(-(\omega\sigma_z/c)^2\right)$. The maximum amount of power deposited in a single RF finger has also been estimated; it is different for different RF fingers. In Fig. 5, the distribution of losses is shown for rf fingers of 1/8 of the total geometry. RF finger number 1, as is shown in Fig. 5, has the maximum loss of about 65 mW which is about 0.5 % of the total power loss. RF finger number 8 shows the minimum loss, about 13 mW. RF fingers are made of copper-beryllium alloy and have only 5 µm silver-coating but, since the skin-depth in silver at the frequency of the mode is about 2 µm, silver conductivity has been taken for the loss calculation. In case of damage (or complete disappearance) of the silver-coating, the conductivity of the copper-beryllium alloy must be used – this roughly doubles the RF finger losses.

TABLE 1. Parameters of two dominant monopole modes.

Parameter name	Monopole mode 1	Monopole mode 2
Frequency: f [GHz]	0.6	1.25
Quality factor: Q	136	890
Shunt impedance: r_l [Linac-Ω]	13.6	2380
Loss factor: k_l [V/nC]	0.13	5.2
Power losses: P_{loss} [W]	2.3	13

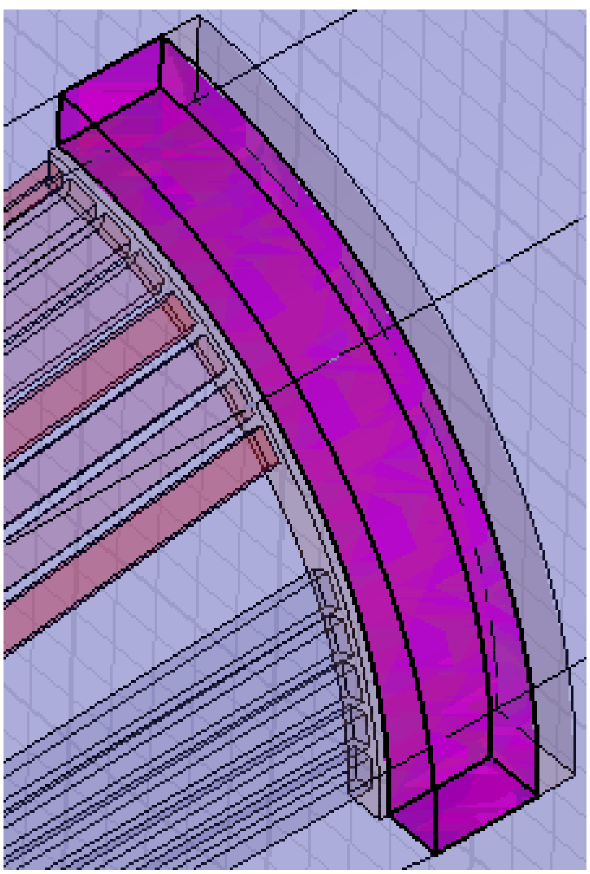

a)

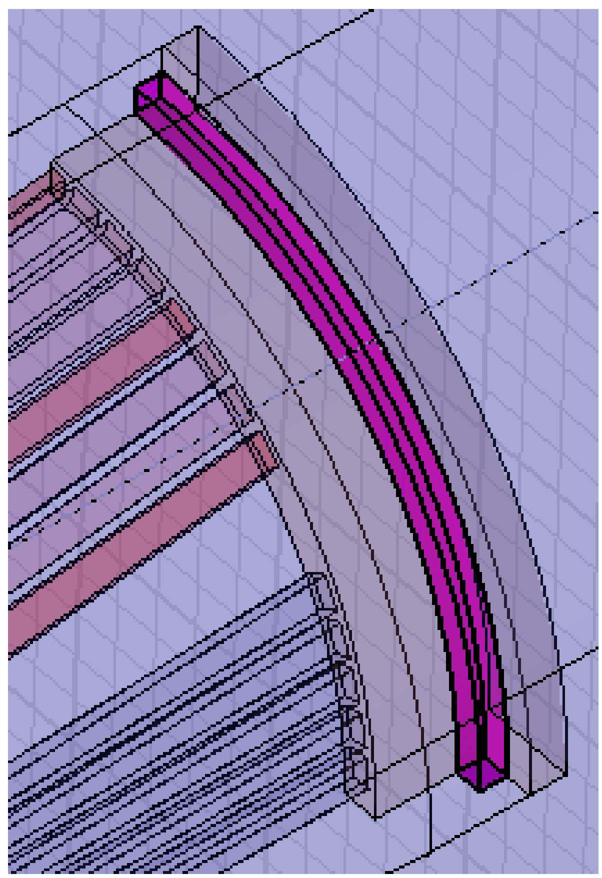

b)

FIGURE 5. Absorbing material placed in the rf finger region for damping the second mode for two different sizes of the ring cross-section: 11 mm x 6 mm in (a) and 3 mm x 3 mm in (b).

Damping of the second mode at 1.25 GHz, which is the most dangerous one, has been investigated as well. Since the field of this mode is concentrated in the transition region (see Fig. 4(b)), absorbing materials must also be placed in the region near the RF fingers, where not much space is available. The only place where absorbing material can be placed without changing the collimator design has been found between the ring holding the RF fingers and the vacuum tank as is shown in Fig. 6. Two different absorbing materials have been investigated: SiC ($\varepsilon = 13$, $\tan\delta = 0.5$ at 2 GHz) and ferrite 4S60 ($\varepsilon = 12 + i7$, $\mu = 1.6 + i9$ at 1.2 GHz [5]). The SiC ring of 11 mm x 6 mm cross-section shown in Fig. 6(a) reduces the mode *Q*-factor from 890 to 17. Though this is already good damping, the ferrite is much better. The ferrite 4S60 ring of only 3 mm x 3 mm shown in Fig. 6(b) reduces *Q*-factor from 890 to 8, and a 6 mm x 6 mm ring of the same material damps the mode completely. The reason for the much better performance of ferrite is not only the higher losses, but also the fact that it magnetic losses dominate, as opposed to dielectric losses in SiC. This is advantageous because the absorbing material is placed in the region of high magnetic field where ferrites work more effectively. The reduction in *Q*-factor by factor 100 reduces power losses presented in Table 1 by about the same amount. The resulted power loss which is negligibly small takes place mainly in the absorber. Moreover, since the absorber is not seen by the beam directly and is not subject to beam image currents there are no other losses.

TRANSVERSE IMPEDANCE OF DIPOLE MODES

Appling a perfect magnetic wall ($H_t = 0$) boundary condition on $x = 0$ and perfect electric wall ($E_t = 0$) one on $y = 0$ symmetry planes of the collimator geometry presented in Fig. 1, dipole modes ($m = 1$) have been calculated. First, the effective transverse impedance, i.e. the impedance taking into account coupling to the Gaussian bunch of 80 mm RMS length, has been calculated using GdfidL for about 10 different values of the gap between collimator plates from 5 mm to 60 mm. In Fig. 7, a map of the real part of the effective transverse impedance is presented in the range of frequencies from DC to 3 GHz and in the range of gap widths from 5 mm to 60 mm. The transverse impedance map also shows two dipole modes at about 0.6 GHz and 1.25 GHz which have similar field distributions to the corresponding monopole modes described in the previous section. In addition, a number of dipole modes in the frequency range from 1.6 GHz to 2 GHz are excited by the beam. Once their frequencies were known, the electromagnetic fields and parameters of the dominant transverse modes have been calculated using HFSS for a gap width of 5 mm. In Fig. 8, transverse impedance of these modes versus frequency is presented in logarithmic scale. Four different types of modes can be distinguished based on their electromagnetic field distribution: low frequency tank modes, transition modes, gap modes, and high frequency tank modes. In Figs. 9 to 11, the electric field distribution of some of these modes is shown for a gap width of 5 mm.

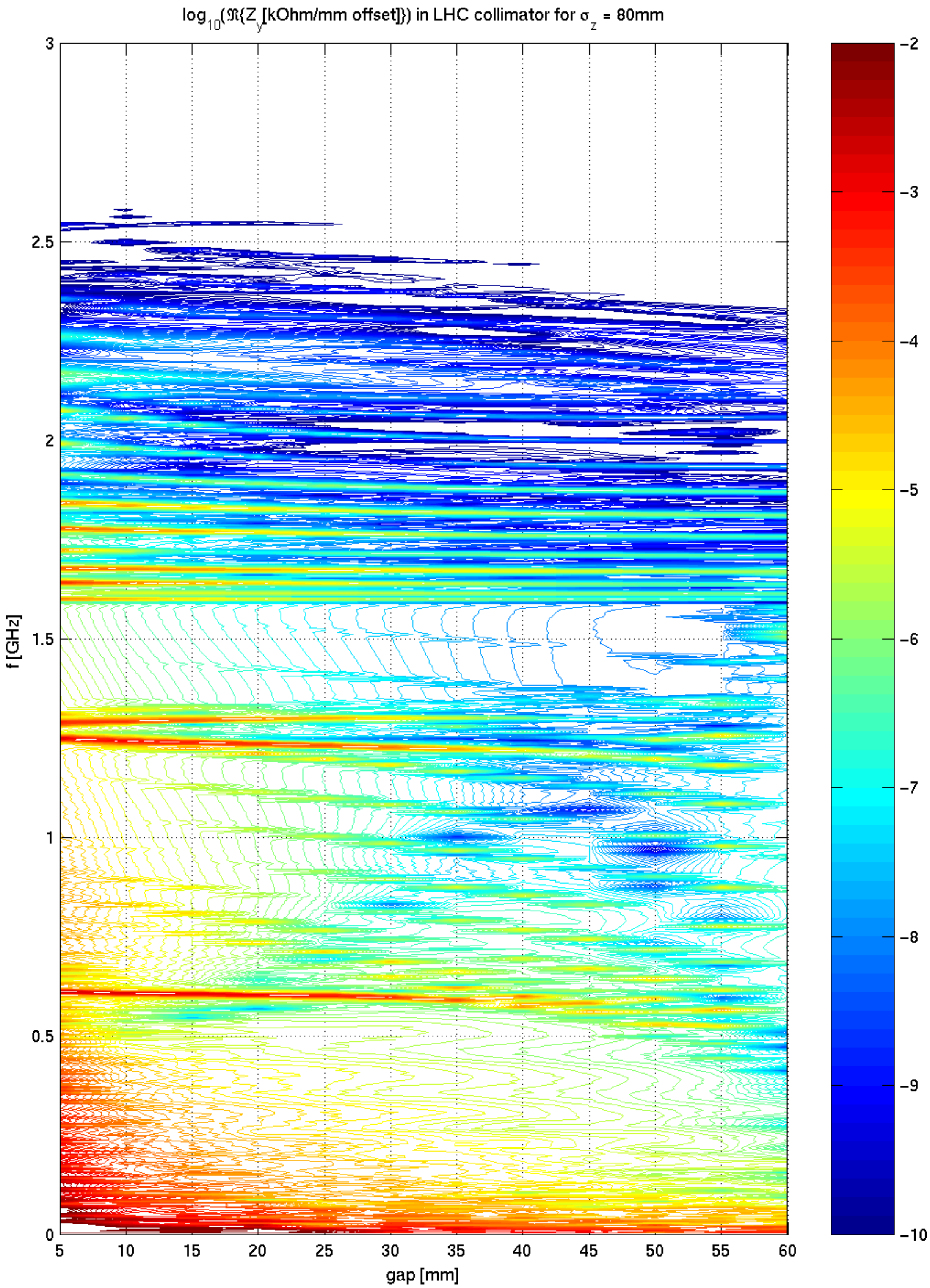

FIGURE 7. Map of effective transverse impedance is presented in the range of frequencies from DC to 3 GHz and in the range of gaps from 5 mm to 60 mm.

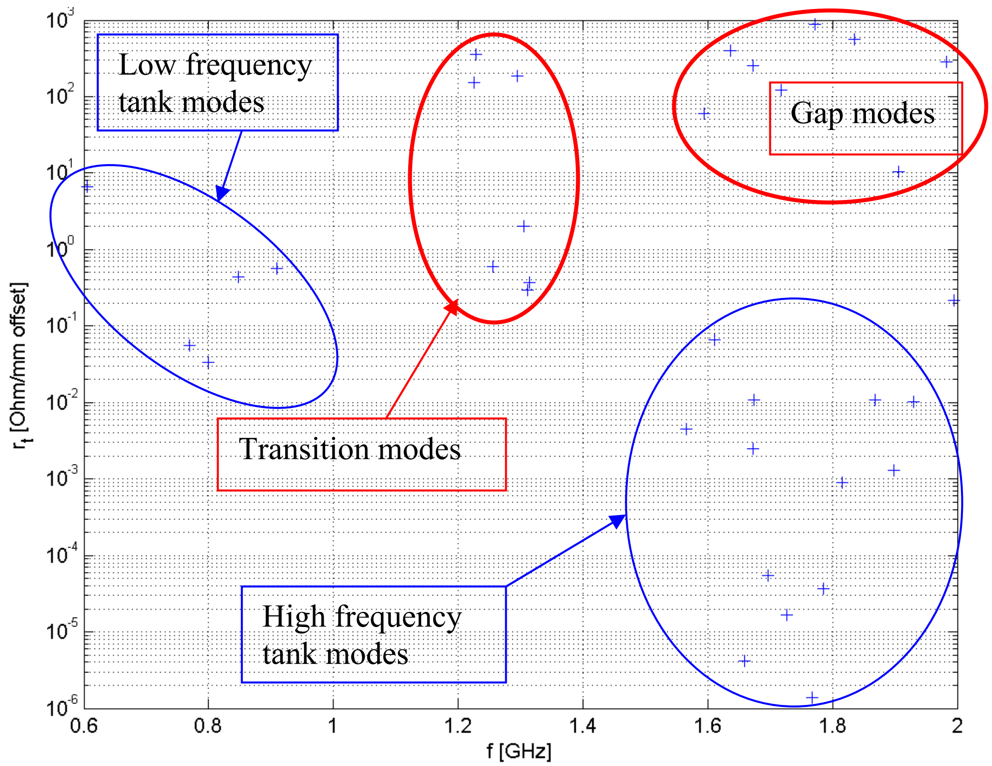

FIGURE 8. Transverse impedance of dipole modes is presented for gap of 5 mm. Different types of modes are shown (see text).

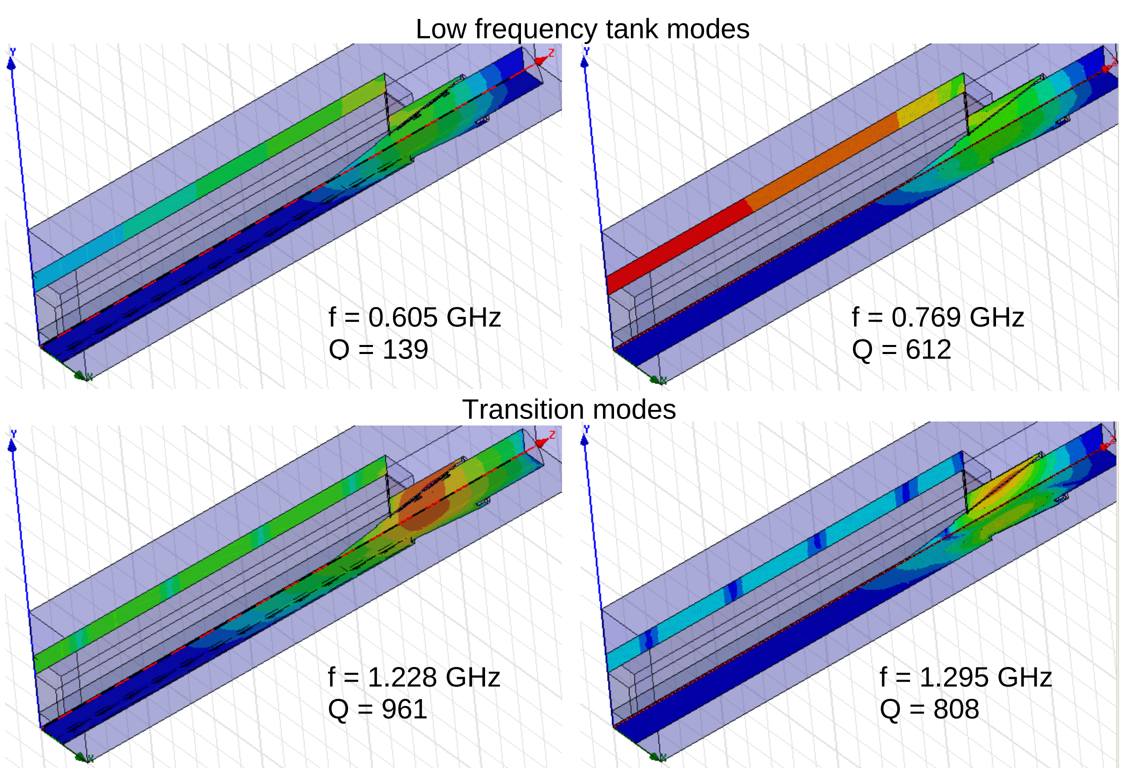

FIGURE 9. Electric field distribution of some of the low frequency tank modes and the transition modes.

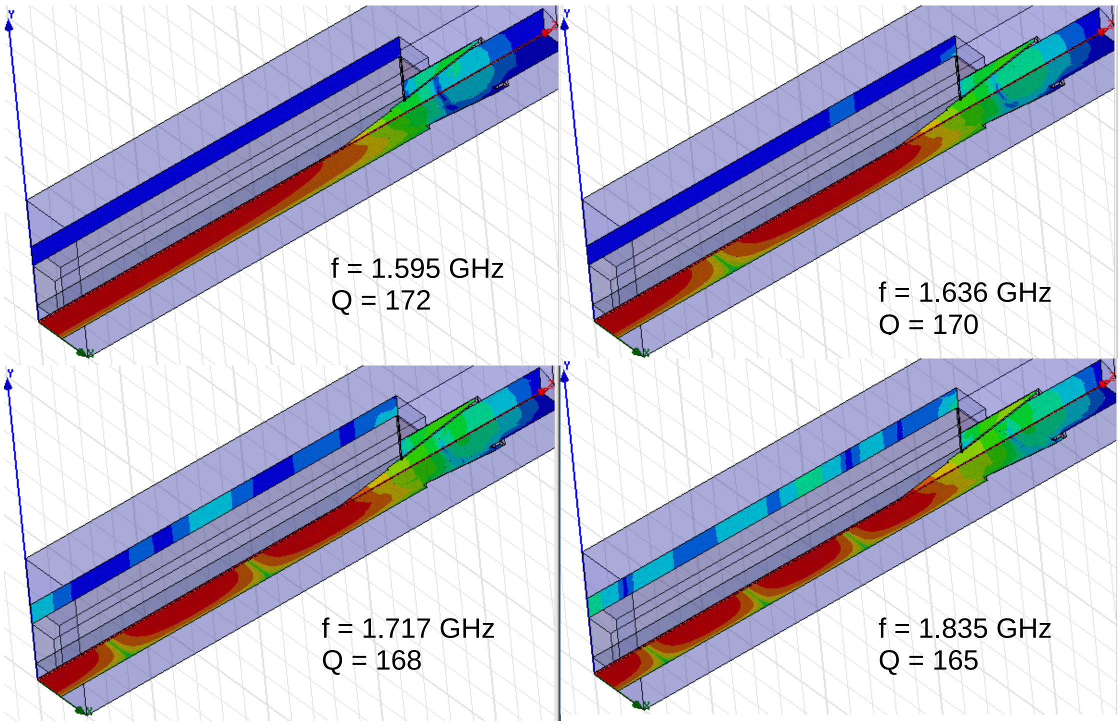

FIGURE 10. Electric field distribution of some of the gap modes.

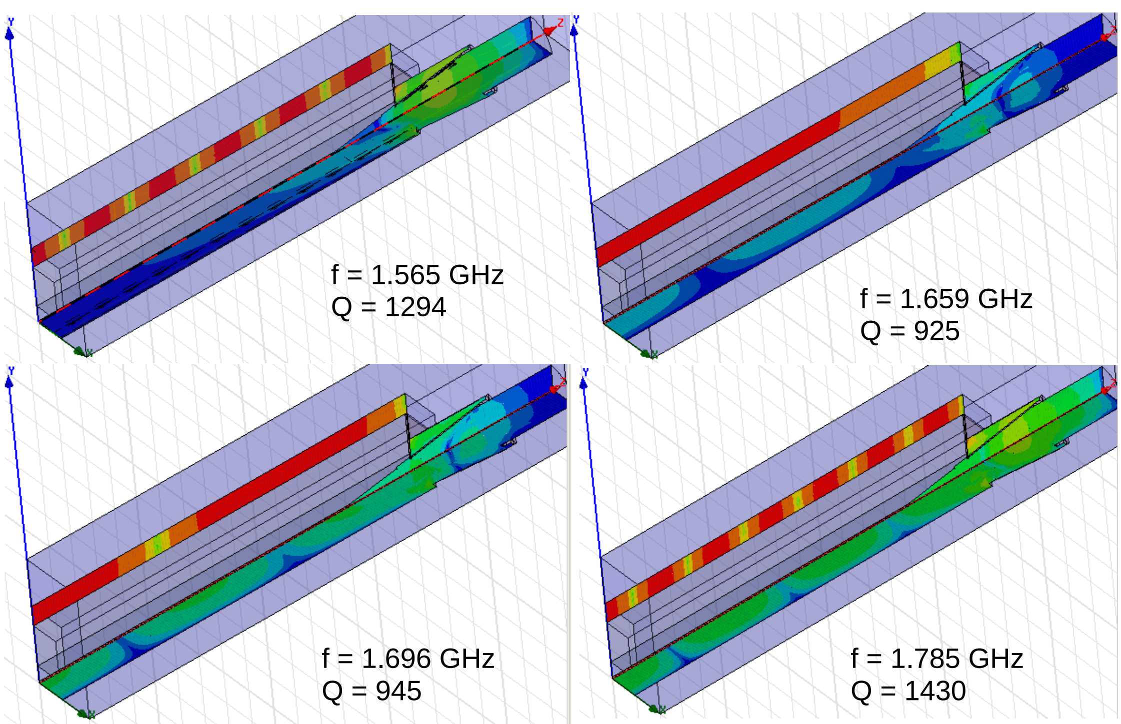

FIGURE 11. Electric field distribution of some of the high frequency tank modes.

TABLE 2. Parameters of the dominant dipole modes for 5 mm gap and for 2.5 mm gap.

#	f_y [GHz]		Q		r_y [LinacΩ/mm]		k_y [V/nC/mm]	
	5mm	**2.5mm**	**5mm**	**2.5mm**	**5mm**	**2.5mm**	**5mm**	**2.5mm**
1	0.605	0.607	140	140	6.7	6.7	0.045	0.046
2	1.226	1.237	930	940	151.7	114.6	0.313	0.237
3	1.228	1.238	960	990	352.5	582.4	0.708	1.144
4	1.295	1.297	810	830	184.5	218.3	0.464	0.536
5	1.306	1.311	570	600	2.0	0.65	0.007	0.002
6	1.595	1.591	172	88	59.6	86.35	0.868	2.452
7	1.611	1.606	171	88	0.06	8.13	0.001	0.233
8	1.636	1.632	170	87	398.2	660.2	6.019	19.45
9	1.672	1.668	169	86	254.1	229.3	3.949	6.985
10	1.717	1.714	168	86	121.5	366.3	1.951	11.47
11	1.772	1.769	167	85	875.9	1342.8	14.60	43.90
12	1.835	1.834	165	84	565.6	619.6	9.881	21.25
13	1.906	1.906	164	83	10.3	6.4	0.188	0.23
14	1.983	1.986	164	83	288.2	618.3	5.474	23.24

The transition modes and the gap modes are dominant since they have the strongest coupling to the beam, their electric field being concentrated near the axis. The parameters of these modes are presented in Table 2 for two values of the gap width, 5 mm and 2.5 mm. Here r_y is transverse impedance in Ω (Linac definition) per mm offset: $r_y = 4k_y Q/\omega_y$, where $\omega_y = 2\pi f_y$ and

$$k_y = c\left(\int_0^L \frac{\partial E_z}{\partial y} e^{j\frac{\omega_y z}{c}} dz\right)^2 \Big/ 4U\omega_y = \omega_y\left(\int_0^L (E_y + cB_x) e^{j\frac{\omega_y z}{c}} dz\right)^2 \Big/ 4U\,c \qquad (1)$$

is the transverse kick-factor, which was calculated in two different ways as is shown in (1). The difference between these two values gives a good indication of the numerical accuracy in the transverse impedance calculation and was found to be below 1 % for the dominant modes. The circuit definition of transverse impedance $Ry = r_y/2$ is usually used to reconstruct impedance versus frequency curve according to equivalent resonant circuit model:

$$Z_y(f) = \frac{R_y}{1 + jQ(f/f_y - f_y/f)}. \qquad (2)$$

In Fig 12, the real part of (2) is plotted in blue for 5 mm gap taking into account 11 of the 14 modes presented in Table 2. The red solid line represents the transverse impedance calculated using GdfidL. The blue and red lines agree very well below 2 GHz where we have found all relevant modes and obviously disagree above 2 GHz where GdfidL shows the existence of higher frequency dipole modes which have not been analyzed in HFSS. On the other hand, the effective impedance of these higher frequency modes is significantly reduced due to the frequency dependence of the form-factor of a Gaussian bunch of 80 mm RMS length $\exp\left(-(\omega\sigma_z/c)^2\right)$ which is plotted in green. Just to get an idea of the order of magnitude of this effect, the transverse impedance of the trapped modes is of the same order of magnitude (~10^5 Ω/m) as the resistive wall transverse impedance of the collimator Graphite plates in the frequency range from 1.6 GHz to 2 GHz [6].

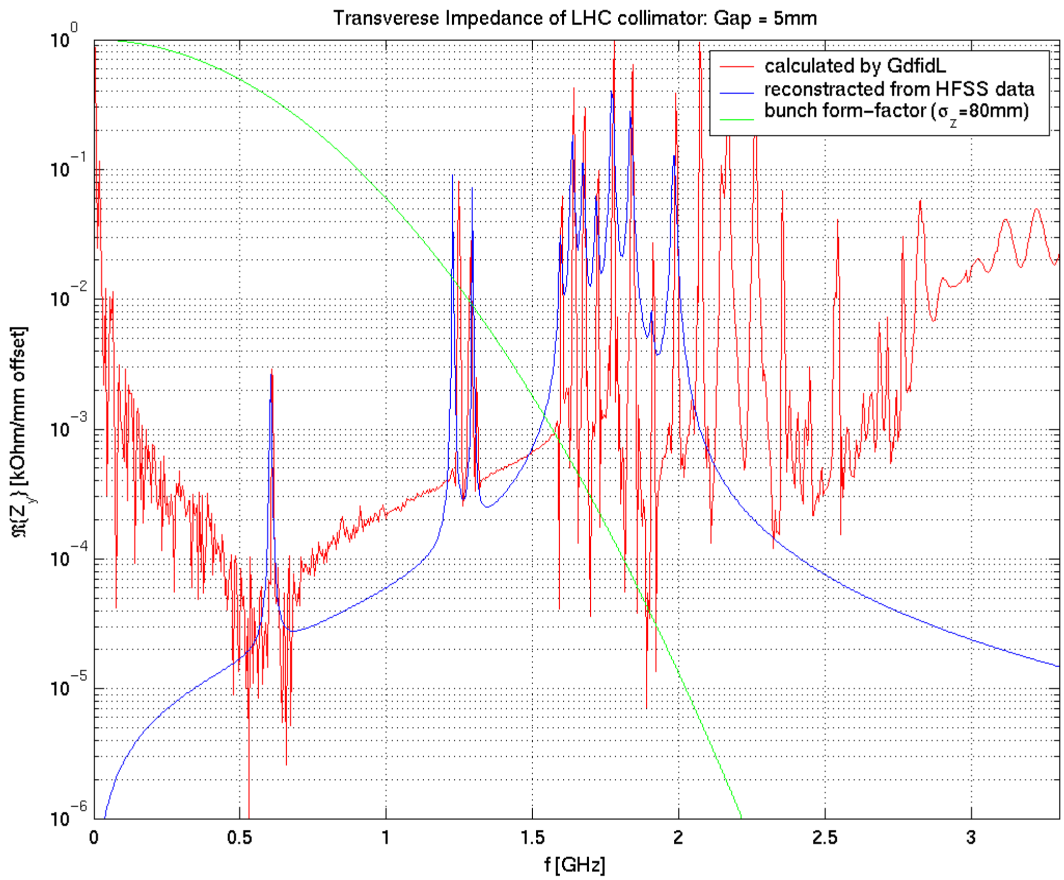

FIGURE 12. Transverse impedance versus frequency of the dipole modes reconstructed from the parameters calculated using HFSS (blue) and calculated using GdfidL (red) is presented for 5 mm gap. Green line shows frequency dependence of the form-factor of a Gaussian bunch of 80 mm RMS length.

CONCLUSIONS

Longitudinal and transverse impedances of the collimator trapped modes have been calculated. The longitudinal impedance results mainly in heating of the collimator. The estimated heating power for the nominal LHC beam is 13 W for the dominant trapped mode. The maximum power per RF finger is 65 mW, which can be doubled in the case of disappearance of the silver-coating. Damping of the dominant monopole mode is possible by placing absorbing material in the region of RF fingers to beam pipe transition. The transverse impedance of the trapped modes is of the order of the resistive wall transverse impedance (~10^5 Ω/m) in the frequency range 1.6 GHz to 2 GHz.

REFERENCES

1. A. Bertarelli et al., LHC Project Report 786, 2004.
2. G. Arduini et al., LHC Project Report 831, 2005.
3. www.ansoft.com
2. www.gdfidl.de
5. F. Caspers (private communication).
6. F. Caspers et al., CERN-AB-2004-065, 2004.